POLYPUBLIE
Polytechnique Montréal

POLYTECHNIQUE MONTRÉAL
UNIVERSITÉ D'INGÉNIERIE

Titre: Title: General relativity: an erfc metric

Auteurs: Authors: Réjean Plamondon

Date: 2018

Type: Article de revue / Article

Référence: Citation: Plamondon, R. (2018). General relativity: an erfc metric. Results in Physics, 9, 456-462. https://doi.org/10.1016/j.rinp.2018.02.035

Document en libre accès dans PolyPublie
Open Access document in PolyPublie

URL de PolyPublie: PolyPublie URL: https://publications.polymtl.ca/3572/

Version: Version officielle de l'éditeur / Published version
Révisé par les pairs / Refereed

Conditions d'utilisation: Terms of Use: CC BY-NC-ND

Document publié chez l'éditeur officiel
Document issued by the official publisher

Titre de la revue: Journal Title: Results in Physics (vol. 9)

Maison d'édition: Publisher: Elsevier

URL officiel: Official URL: https://doi.org/10.1016/j.rinp.2018.02.035

Mention légale: Legal notice:

Ce fichier a été téléchargé à partir de PolyPublie, le dépôt institutionnel de Polytechnique Montréal
This file has been downloaded from PolyPublie, the institutional repository of Polytechnique Montréal

https://publications.polymtl.ca

Results in Physics 9 (2018) 456–462

Contents lists available at ScienceDirect

Results in Physics

journal homepage: www.journals.elsevier.com/results-in-physics

General relativity: An *erfc* metric

Réjean Plamondon

Département de Génie Électrique, École Polytechnique de Montréal, Montréal (Québec) H3C 3A7, Canada

ARTICLE INFO

Article history:
Received 21 December 2017
Received in revised form 16 February 2018
Accepted 17 February 2018
Available online 23 February 2018

ABSTRACT

This paper proposes an *erfc* potential to incorporate in a symmetric metric. One key feature of this model is that it relies on the existence of an intrinsic physical constant σ, a star-specific proper length that scales all its surroundings. Based thereon, the new metric is used to study the space–time geometry of a static symmetric massive object, as seen from its interior. The analytical solutions to the Einstein equation are presented, highlighting the absence of singularities and discontinuities in such a model. The geodesics are derived in their second- and first-order differential formats. Recalling the slight impact of the new model on the classical general relativity tests in the solar system, a number of facts and open problems are briefly revisited on the basis of a heuristic definition of σ. A special attention is given to gravitational collapses and non-singular black holes.

© 2018 The Author. Published by Elsevier B.V. This is an open access article under the CC BY-NC-ND license (http://creativecommons.org/licenses/by-nc-nd/4.0/).

Introduction

The idea of modifying gravity to come up with new relativistic field descriptions is not new and several approaches have been proposed in that direction over the years [1–4]. Indeed, the extension of gravity to correct and enlarge Einstein theory has been proposed time and again over the last thirty years to take into account several shortcomings of the theory when cosmological, astrophysical, mathematical and quantum mechanical observations and objections are taken into account [5–7]. In this context, we propose in this paper a phenomenologically possible modification of Newton's gravity using an *erfc* potential as the gravitational source of space–time curvature. In the next section, the resulting metric is put forward and briefly described. In Section "Analysis of a symmetric system", using the standard relativistic procedure, we introduce and analyze a new symmetric metric. One key feature of this model is that it relies on the existence of an intrinsic physical constant σ, a star-specific proper length that scales all its surroundings. The main predictions of this *erfc* metric are the two types of departures from a Schwarzchild's geometry: a constant offset that spreads all over the manifold and an *erf* term slightly smaller than the classical r^{-1} function. Although σ is an experimental parameter, we use in Section "A heuristic estimate of σ", a heuristic approach to estimate it and define a star's proper length. We analyze the impact of the resulting deviations on the classical general relativity tests and we point out how they could provide partial explanations to open problems in the solar system or reinterpretations of well-known observations made from this system. We particularly focus on the numerical origin of the Hubble Constant. Then, in Section "Curvature Sensors", taking a more global perspective, we present a brief analysis of the field equations resulting from the new metric and of the geodesics for the motions of massive particles and photons for a Sun-like environment. Lastly, in S ection "Gravitational collapse", we briefly revisit gravitational collapse and black holes and in Section "Discussion", prior to conclusion, we point out some open problems where the new metric could be brought into play to investigate prospective solutions.

An *erfc* potential

In the context of the fifth force hypothesis, several minor modifications have been proposed as possible violations of Newtonian gravity. Although the concept of the fifth force has been put aside [8], the idea of modifying gravity is still on the agenda [9]. Another motivation for publishing the present paper is to look for a geometry that would soften or remove singularities appearing in General Relativity at short distances. One interesting function that reduces to the Newton potential and that has been recently proposed [10], is the following:

$$\Phi_{erfc}(r) = GM\left(\frac{\sqrt{\pi}}{\sigma\sqrt{2}}\right)erfc\left(\frac{\sigma}{\sqrt{2}r}\right) = GM\left(\frac{\sqrt{\pi}}{\sigma\sqrt{2}}\right) - GM\left(\frac{\sqrt{\pi}}{\sigma\sqrt{2}}\right)erf\left(\frac{\sigma}{\sqrt{2}r}\right) \quad (1)$$

Indeed, since

$$-GM\left(\frac{\sqrt{\pi}}{\sigma\sqrt{2}}\right)erf\left(\frac{\sigma}{\sqrt{2}r}\right) = -GM\left(\frac{1}{r} - \frac{\sigma^2}{6r^3} + \frac{\sigma^4}{40r^5} - \dots\right) \cong -\frac{GM}{r} \quad (2)$$

E-mail address: rejean.plamondon@polymtl.ca

https://doi.org/10.1016/j.rinp.2018.02.035
2211-3797/© 2018 The Author. Published by Elsevier B.V.
This is an open access article under the CC BY-NC-ND license (http://creativecommons.org/licenses/by-nc-nd/4.0/).

the *erfc* potential converges, to a gauge factor, near the Newtonian limit at large r values. In classical mechanics, this gauge factor is arbitrarily fixed to zero. In the present study, we link it to a parameter σ that defines what we will refer to as the proper length of the massive object generating this potential.

The resulting field is thus given by:

$$\vec{g}(r) = -\vec{\nabla}\Phi_{erfc}(\mathrm{r}) = -\frac{GM}{r^2}\exp\left(-\frac{\sigma^2}{2r^2}\right)\vec{u}_r \tag{3}$$

which also reduces to the Newton description for large r values, since the exp factor tends toward unity under this condition. Eq. (3) can also be interpreted as assuming a variable G.

In other words, Eq. (1) predicts a constant non-null potential at $r = \infty$ and its radial component converges towards the Newton limit, if the constant term included in the *erfc* function is arbitrarily subtracted, which leads to an *erf* potential that tends towards a $1/r$ behaviour at large r. These are the particular features of an *erfc* potential which leads to an original description of the spacetime surrounding a massive object as seen below.

Analysis of a symmetric system

The metric

If the *erfc* potential is incorporated into a metric describing a static symmetric massive object, the following line element is obtained:

$$ds^2 = \left[1 + \frac{2K_\sigma}{c^2}erfc\left(\frac{\sigma}{\sqrt{2}r}\right)\right]c^2dt^2 - \left[1 + \frac{2K_\sigma}{c^2}erfc\left(\frac{\sigma}{\sqrt{2}r}\right)\right]^{-1}dr^2 - r^2d\theta^2 - r^2\sin^2\theta d\phi^2 \tag{4}$$

where the constant $K_\sigma = \sqrt{\pi}GM/\sigma\sqrt{2}$ has been introduced for simplification purposes. This metric has no intrinsic nor coordinate singularity. We develop the various field solutions in Section "Curvature tensors" i.e. the equations for the $R_{\mu\nu}$, $G_{\mu\nu}$, the Ricci and Kretschman scalars as well as the second- and first-order geodesics. All these curves converge towards zero near the centre of the star since the matter energy density decreases drastically as the volume of the encapsulating sphere vanishes as $r \to 0$. These geodesics can be used to study the movements of test particles of unitary mass and of photons, following the standard procedure [10].

It should be noted that two types of corrections are predicted by the *erfc* potential, as compared to Einstein's results: one is due to the constant offset associated with the definition of the *erfc* and the other to the difference between an *erf* potential and Newton's $1/r$ law. More specifically, the offset induces constant errors in distance or time measurements as compared to no offset, while the error between a Newtonian and an *erf* potential is of the order of $\frac{\sigma^2}{6r^3}$, which might be negligible or not, depending on the experimental value of σ. At large distances, when the offset effect is neglected, the study of radial trajectories and equatorial orbits converges towards Einstein's predictions.

Masking the constant offset potential

Regarding the *erfc* offset, which is quite specific to this metric, differences appear when the energy associated with it is taken into account. A way to point this out is to look at a metric that neglects this hidden energy [11].

One practical way for an observer to partly neglect the constant gauge associated with the *erfc* potential is to remove it from the metric set out in Eq. (4) and incorporate its effect by an increase of the theoretical value of the speed of light used in the model, making sure that, at infinity, in a flat space–time, the length element ds^2 will not be affected:

$$\left[1 + \frac{2K_\sigma}{c_{th}^2}\right]c_{th}^2dt^2 - \left[1 + \frac{2K_\sigma}{c_{th}^2}\right]^{-1}dr^2 = c_d^2dt^2 - dr^2 = 0, when\ r \to \infty. \tag{5}$$

where the subscript *th* and *d* stand respectively for the theoretical and the defined value of the speed of light. For a photon, $ds^2 = 0$ and, keeping the same coordinates, Eq. (5) leads to a quadratic relationship between σ, c_{th} and c_d:

$$c_{th}^2 - c_dc_{th} + 2K_\sigma = 0 \Rightarrow \frac{c_d}{c_{th}} = \left[1 + \frac{\sqrt{2\pi}GM}{c_{th}^2\sigma}\right] \tag{6}$$

where the right-hand part is obtained after a division by c_{th}^2 and the substitution of K_σ by what it stands for.

In other words, according to this model, an observer working with a defined value c_d of the speed of light in a flat space–time will mask the effect of the constant offset and its local measurements in flat space will not be affected. However, using this masking scheme to study a curved space–time is equivalent to working with an *erf* potential, at the price of using a metric with an intrinsic singularity at $r_{\mathrm{int}.sing} = 0$ and a coordinate singularity, at:

$$erf\left(\frac{\sigma}{\sqrt{2}r_{\mathrm{coord}.sing}}\right) = \frac{c_d^2}{2K_\sigma} \tag{7}$$

These singularities are not present in the original metric set out in Eq. (4). Another problem with this making strategy is that, for an observer keeping the same coordinates, the *erfc* and the *erf* metrics will not be fully equivalent in a curved space, when $r \neq \infty$:

$$\begin{aligned} ds^2 &= \left[1 + \tfrac{2K_\sigma}{c_{th}^2} - \tfrac{2K_\sigma}{c_{th}^2}erf\left(\tfrac{\sigma}{\sqrt{2}r}\right)\right]c_{th}^2dt^2 - \left[1 + \tfrac{2K_\sigma}{c_{th}^2} - \tfrac{2K_\sigma}{c_{th}^2}erf\left(\tfrac{\sigma}{\sqrt{2}r}\right)\right]^{-1}dr^2 \\ &\neq \left[1 - \tfrac{2K_\sigma}{c_{th}^2}erf\left(\tfrac{\sigma}{\sqrt{2}r}\right)\right]c_d^2dt^2 - \left[1 - \tfrac{2K_\sigma}{c_{th}^2}erf\left(\tfrac{\sigma}{\sqrt{2}r}\right)\right]^{-1}dr^2 \end{aligned} \tag{8}$$

since the *erf* terms of the time components are weighted differently. For measurements based on photons, there will be a systematic error resulting from the difference between these two expressions:

$$dt = \frac{dr}{[c_d^2 - c_{th}^2]^{1/2}\left[1 + \frac{2K_\sigma}{c_{th}^2}erfc(\frac{\sigma}{\sqrt{2}r})\right]^{1/2}\left[1 - \frac{2K_\sigma}{c_{th}^2}erf\left(\frac{\sigma}{\sqrt{2}r}\right)\right]^{1/2}\left[erf\left(\frac{\sigma}{\sqrt{2}r}\right)\right]^{1/2}} \tag{9}$$

Here again the experimental value of σ will be a determining factor in evaluating this bias. For relatively small values of σ, this *erf* potential can be considered as a perturbation that induces orbital effects which could be calculated analytically according to techniques like the Lagrange planetary equations and the results compared for example with the most recent observational determinations from Solar System data. In this way, it would be possible to extract preliminary upper bounds on σ. Leaving these issues open for the moment, we present in Section "A heuristic estimate of σ", a few typical predictions that emerge from a heuristic estimate of σ to highlight the interest of taking the full *erfc* potential into account and push on further along this direction.

A heuristic estimate of σ

The range parameter σ is a global empirical factor, a proper length specific to a given star. It should be measured experimentally to study its effect in a particular environment. Nevertheless, as already explained in Plamondon (2017) [12], we can estimate

it in order to highlight the interest of exploring this avenue and making some numerical predictions. Here is how it goes. We take a bulk approach, in the Newtonian limit, to mimic what historically happened on Earth when the metric system was defined, but we take on a more general and unit independent approach first, to make a comprehensive estimation of σ.

An observer living on a planet P orbiting a star S of mass M_S and radius r_S has defined a reference length unit l_{ref} and used a fraction y of this length to define a reference volume $(yl_{ref})^3$. He has poured in this volume a quantity x of a substance s_1, to establish a macroscopic unit of mass u_m. He then has defined a local volumetric mass reference density ρ_{ref} using the selected quantity x of the arbitrary reference substance s_1. Working with 3-ball volume in accordance with the extrinsic Newtonian description of the world instead of the intrinsic 2-sphere projections used in general relativity, he proposes the following heuristic to estimate the proper length σ_P of his planet:

$$\sigma_P \frac{4\pi r_P^2}{(4/3)\pi r_P^3} = \left[\frac{\rho_{ref}}{\rho_P}\right]\left[\frac{u_m}{m_{s1}}\right] \Rightarrow \sigma_P = \frac{r_P \rho_{ref} u_m}{3\rho_P m_{s1}} \tag{10}$$

As a result, σ_P is assumed to be inversely proportional to the planet mean density ρ_S as defined with respect to the reference density ρ_{ref} and inversely proportional to the mass of the arbitrary reference substance m_{s1}, as defined with respect to u_m and used to define the reference density. Moreover σ_P should be weighted by the 2-sphere surface defined by the time and radial components of the metric to the corresponding 3-ball volume ratio embedded in this 2-sphere, to be consistent with the extrinsic Newtonian descriptions. According to this heuristics, the proper length, σ, associated with any massive object will be larger when the object radius is larger, smaller for larger relative mean density and weighted by the ratio of the unit of mass to the mass of the reference substance m_{s1} used to define the reference density ρ_{ref}.

For example, an observer living on Earth, working in SI units, that is using $l_{ref} = 1$ m and $u_m = 1$ kg where 1 kg corresponds to the mass of 1 dm^3 of water which leads to $m_{s1} = m_{H_2O} = 18.01528(30)u_m$, $r_E = 6.378137(2) \times 10^6$m, $\rho_{ref} = 1000$ kg/m^3 $\frac{\rho_E}{\rho_{ref}} = 5.5140(6)$, will get from Eq. (10) an estimate of:

$$\sigma_E = 2.1298(2) \times 10^4 \text{m} \tag{11}$$

and, using Eq. (6), the corresponding two roots c_{th1} and c_{th2}:

$$\begin{aligned} c_{th1} &= c_{thE} = 299792302\ (.02)\ \text{m/s} \\ c_{th2} &= \Delta c_E = c_d - c_{th1} = 156\ (.02)\ \text{m/s} \end{aligned} \tag{12}$$

Putting the value of σ_E in Eq. (3) the maximal difference in the modified field value as compared to Newton's predictions, in a range of 500 m above the Earth surface, is of the order of 54.6 μGal, using $G = 6.67408(31) \times 10^{-11}$ m^{3}kg^{-1}s^2 [13], $M_E = 5.9722(6) \times 10^{24}$ kg [14] and $r_E = 6.378137 \times 10^6$ m, which is in the range of the associated errors reported for various tower experiments as summarized in [15,16] in the context of an eventual fifth force interpretation [8]. The difference of the difference between the theoretical predictions at 500 m as compared to the sea level is negligible, around 0.003 μGal.

For the Sun, $r_{Sun} = 6.9551(4) \times 10^8$ m, $\frac{\rho_{Sun}}{\rho_{ref}} = 1.4111(2)$, this general model leads to:

$$\begin{aligned} &\sigma_{Sun} = 9.1508(20) \times 10^6\ \text{m} \\ &c_{th1} = c_{thSun} = 299671152(27)\text{m/s} \\ &c_{th2} = 121306(27)\text{m/s} \\ &c_d = c_{th1} + c_{th2} = 299792458\text{m/s} \\ &\Rightarrow c_{th2} = \Delta c_{Sun} = c_d - c_{th1} \end{aligned} \tag{13}$$

The heuristics (10) also suggests that it is not at very small distance experiments that the departure from Newton's law will be revealed. Indeed, the main radial correction factor between a Newtonian and an *erfc* potential $\frac{\sigma^2}{6r^3}$ is very small for microscopic local tests of gravity, according to Eq. (10). To give a simple numerical example, in their most recent study, Yang et al. [17] used a tungsten plate of $15.994 \times 15.986 \times 1.787$ mm^3 $= 772.458$ mm^3 as a source mass of 1.487×10^{-2} kg. If we convert this mass into an equivalent sphere of radius 5.692×10^{-2} m, using the tungsten density (19.250 kg/m^3), the resulting value $\sigma = 5.471 \times 10^{-5}$ m will lead to a correction of 2.705×10^{-6} m^{-1}, which is beyond the technological limits of observation.

Similarly, at the Earth position in the solar system, the correction is at or beyond the limits of the present technology [18] in many experiments. Indeed, assuming that the ansatz defined by (10) is valid, it has been shown that the effects of the *erfc* potential will be slightly apparent in the solar system with regards to the classical test of general relativity. On the one hand, the *erf* perturbation effects can be assumed to be negligible at large r; for example, on the Earth orbit, $\frac{\sigma^2}{6r^3} = \frac{(9.1508\times10^6)^2}{6\times(1.495\times10^{11})^3} = 4.13 \times 10^{-21}$ m^{-1} and 7.186×10^{-20} m^{-1} on the Mercury orbit, using its mean radius $r = 5.791 \times 10^{10}$ m. On the other hand, the *erfc* offset will not affect most of the classical tests since the systematic distance errors that result from this offset will be cancelled.

For example, according to Nobili and Will (1986) [19], the 42.98″/cy Mercury precession using Einstein's theory will not be affected since the correction factor $\chi = c_{th}/c_d$ will be applied twice, both to the numerator and the denominator of:

$$\dot{\omega}_{precession} \cong \frac{6\pi k^2}{PD^2\bar{a}(1-e^2)} \frac{A_{th}^2}{c_{th}^2} = \frac{6\pi k^2}{PD^2\bar{a}(1-e^2)} \frac{\chi^2 A_d^2}{\chi^2 c_d^2} = \dot{\omega}_{Einstrein} \tag{14}$$

using the same values, as in [19], for the different parameters.

Similarly, it can be shown that the maximal linear light bending predictions will not be affected either as well as for the radar echoes although a slight impact might be observed on gravitational redshifts and time delays depending on the experimental conditions [12].

However, there are examples where the offset of an erfc potential could provide new insights to some open problems [20].

A specific analysis of some of these solar system anomalies has been recently published [12], linking these to the value of the Hubble constant as predicted by the new metric. Indeed, using the same heuristics (Eq. (10)), the Hubble constant H_0 can be linked to σ_{Sun}. If the difference $\Delta c = c_d - c_{th1} = c_{th2}$ (Eq. (12) between the defined and the theoretical values of the speed of light is expressed as an equivalent systematic redshift in the measurement of a reference wavelength λ_{th1}:

$$\Delta c = \frac{\lambda_d - \lambda_{th1}}{\lambda_{th1}} c_d = \frac{\Delta\lambda}{\lambda_{th1}} c_d \tag{15}$$

for an observer working with c_d in an inertial reference system and exploring the outer space, the cumulative effect of this error over time will be equivalent to a space–time expansion, each space–time event moving away with an intrinsic velocity:

$$V_{\text{exp}} = n\Delta c = \frac{n\Delta\lambda}{\lambda_{th}} c_d \tag{16}$$

where $n = \frac{D}{c_d \delta\tau}$ is the number of times the Δc correction must be applied when a distance D is measured with c_d and $\delta\tau$ is the reference time unit used. According to this model, the light coming from a distant galaxy will be redshifted and the corresponding receding velocity V_{gal} will be:

$$V_{gal} = 2V_{\exp} = \frac{2D}{c_d \delta\tau}\frac{\Delta\lambda}{\lambda_{th}}c_d = \frac{2D\Delta c}{c_d\delta\tau} = \frac{2\Delta c}{D_{ref}}D \tag{17}$$

where D is the galaxy distance and the factor 2 comes from the fact that the observer's galaxy is also receding at $V_{\exp}$. Using the length scale $D_{ref} = 1$ Mpc, Eq. (17) can be rewritten as:

$$3.26V_{\text{gal}} = \frac{2\Delta c}{1\ \text{Mpc}}D_{\text{Mpc}} \tag{18}$$

where the factor 3.26 takes into account the rescaling of the time basis $\delta\tau$ when working in Mpc. Overall this leads to Hubble's Law:

$$V_{\text{gal}} = H_0 D_{\text{Mpc}}$$
$$\text{where } H_0 = \frac{2_{\Delta c}}{3.26\ \text{Mpc}} = 74.42\ (.02)\ (\text{km/s}\cdot\text{Mpc}) \tag{19}$$

This latter numerical estimate is found using $\Delta c = \Delta c_{Sun} = 121306(27)m/s$, as computed from the Sun *erfc* metric and the heuristic estimate of σ_{Sun} using Eq. (12). This is almost identical to the recently updated values of H_0 = 74.2 ± 3.6 km/s·Mpc [21,22] or H_0 = 74.3 ± 1.5 km/s·Mpc [23], H_0 = 73.8 ± 2.4 km/s·Mpc [24] as measured from Doppler shift experiments, or 73.2. 4 ± 1.74 km/s/Mpc as obtained from new near-infrared observations of Cepheid variables [25]. What is of interest here is that the value of the Hubble Constant is Sun dependent. An observer living in the surround of another star would find another value, which ultimately questions the current interpretation of the bigbang [12].

Similarly, as developed in [12], one can link the secular increase of the astronomical unit V_{AU} to σ_E. The accuracy of resulting numerical prediction $V_{\text{AU}} \cong 7.8\ \text{cmy}^{-1}$ calls for more investigations of the *erfc* metric by specific experts. Moreover, regarding the expected impacts of the new metric on the flybys anomalies and the Pioneers delay, it has been shown that both phenomena could be partly taken into account within the context of the present heuristic model, with quite accurate numerical predictions. A correction for the osculating asymptotic velocity at the perigee of the order of 10 mm/s and an inward radial acceleration of $8.34 \times 10^{-10}\ \text{m/s}^2$ affecting the Pioneer space crafts could be explained by this new metric.

What is of interest in the sequel is a detailed investigation of a star spacetime geometry based on the heuristic definition of σ (Eq. (10)), since various non null tensors are predicted by the model, which globally affect the geodesics.

Curvature tensors

The $R_{\mu\mu}$ are all different from zero:

$$R_{00} = -\frac{\alpha c^2 \beta\sigma^2}{r^3}, \tag{20}$$

$$R_{11} = \frac{\beta\sigma^2}{\alpha r^3}, \tag{21}$$

$$R_{22} = (\alpha - 1) + 2r\beta, \tag{22}$$

$$R_{33} = [(\alpha - 1) + 2r\beta]sin^2\theta, \tag{23}$$

as well as the Ricci [26] R_s and the Kretschmann [27] K_r scalars:

$$R_s = -\left[\frac{2\beta\sigma^2}{r^3} + \frac{4\beta}{r} + \frac{2(\alpha-1)}{r^2}\right], \tag{24}$$

$$K_r = \frac{4\beta^2[2r^2 - \sigma^2]^2}{r^6} + \frac{16\beta^2}{r^2} + \frac{4(\alpha-1)^2}{r^4}, \tag{25}$$

where we have defined:

$$\alpha = 1 + \frac{2\Phi}{c^2} = 1 + \frac{2K_\sigma}{c^2}erfc\left(\frac{\sigma}{\sqrt{2}r}\right), \tag{26}$$

and

$$\beta = \frac{GM}{c^2r^2}\exp\left(-\frac{\sigma^2}{2r^2}\right). \tag{27}$$

Similarly, for the $G_{\mu\mu}$:

$$G_{00} = \alpha c^2\left[\frac{2\beta}{r} + \frac{(\alpha-1)}{r^2}\right], \tag{28}$$

$$G_{11} = \frac{-1}{\alpha}\left[\frac{2\beta}{r} + \frac{(\alpha-1)}{r^2}\right], \tag{29}$$

$$G_{22} = \frac{-\sigma^2\beta}{r} \tag{30}$$

$$G_{33} = \frac{-\sigma^2\beta}{r}\sin^2\theta \tag{31}$$

These $R_{\mu\mu}$ and $G_{\mu\mu}$ are depicted in Figs. 1 and 2 while Rs and Kr are sketched in Fig. 3 for the Sun using the heuristics set out in Eq. (13), looking through its equatorial plane at $\theta = \pi/2$. Under these conditions, $R_{22} = R_{33}$ and $G_{22} = G_{33}$ and a single graph has been plotted for both pairs of tensors.

Since the metric has no singularity, none of these curves diverge and the coordinates used to describe the resulting geometry are valid from r equal zero to infinity. The overall attractive effect is depicted by the negative Ricci scalar and the resulting positive tidal forces as illustrated by the Kretschmann local curvature. As previously pointed out, all the curves converge towards zero near the centre of the star.

Looking at the $G_{\mu\mu}$ curves, which is equivalent to looking directly at the momentum-energy tensor of a specific density at a given event, an observer sees that the positive curvature G_{00} associated with the matter-energy density induces a negative radial curvature G_{11} that is, an attractive pressure directed towards the star centre, as well as non-negligible negative angular pressures associated with the angular terms G_{22} and G_{33}.

Geodesics

The geometry of the *erfc* space–time surrounding the previous static symmetric body can be described by the four second-order geodesic equations:

$$\ddot{t} + \frac{2\beta\dot{t}\dot{r}}{\alpha} = 0, \tag{32}$$

$$\ddot{r} + \alpha\beta c^2\dot{t}^2 - \frac{\beta}{\alpha}\dot{r}^2 - \alpha r(\dot{\theta}^2 + \sin^2\theta\dot{\phi}^2) = 0, \tag{33}$$

$$\ddot{\theta} + \frac{2\dot{r}\dot{\theta}}{r} - (\sin\theta\cos\theta)\dot{\phi}^2 = 0, \tag{34}$$

$$\ddot{\phi} + \frac{2\dot{r}\dot{\phi}}{r} + (2cot\theta)\dot{\theta}\dot{\phi} = 0, \tag{35}$$

where $x^\mu = x^\mu(l)$ is an affinely parameterized geodesic, $\dot{x}^\mu \equiv dx^\mu/dl$ and $\ddot{x}^\mu \equiv d^2x^\mu/dl^2$.

For a massive test particle moving in the equatorial plane $\theta = \pi/2$, these equations reduce to:

$$\alpha\dot{t} = k, \tag{36}$$

$$\dot{r}^2 + \frac{h^2\alpha}{r^2} + 2\Phi = c^2(k^2 - 1), \tag{37}$$

$$r^2\dot{\phi} = -h, \tag{38}$$

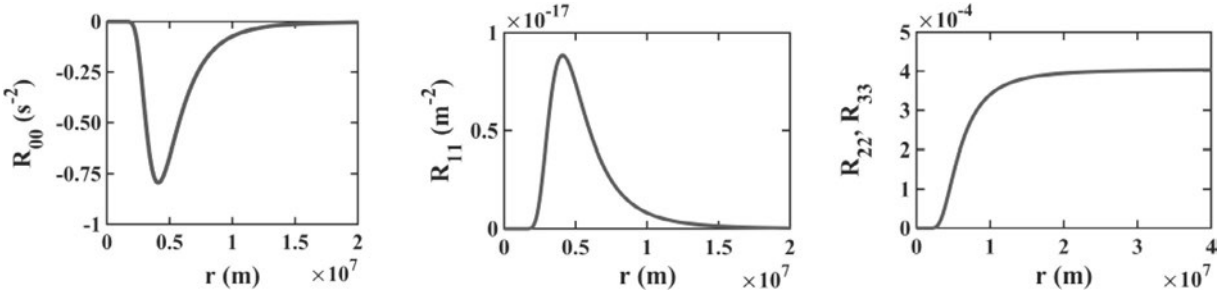

Fig. 1. The $R_{\mu\mu}$ as a function of r, for the symmetric metric. (a) R_{00}, (b) R_{11}, (c) R_{22} and R_{33}.

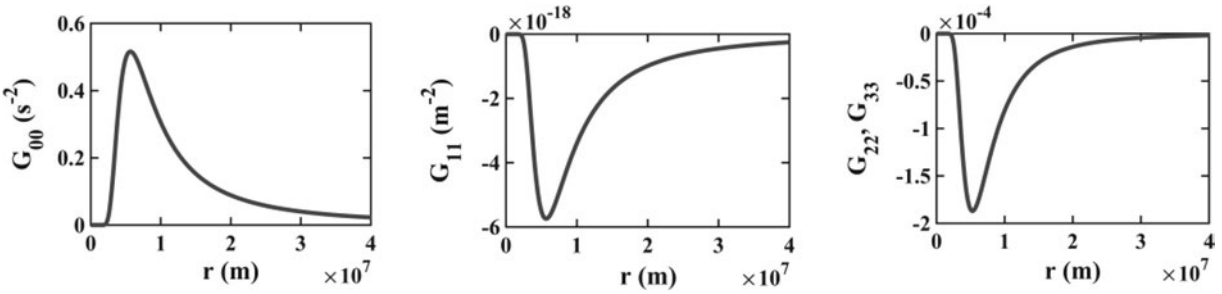

Fig. 2. The $G_{\mu\mu}$ as a function of r, for the symmetric metric. (a) G_{00}, (b) G_{11}, (c) G_{22} and G_{33}.

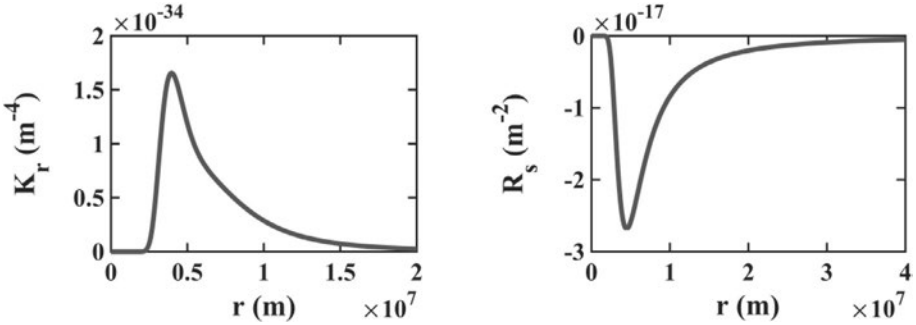

Fig. 3. (a) The Kretschmann local curvature $K_r = R_{\alpha\beta\mu\nu} R^{\alpha\beta\mu\nu}$ and (b) the Ricci scalar R_s as a function of r for the symmetric metric.

where the proper time τ is now taken as the affine parameter ($\dot{x}^\mu \equiv dx^\mu/d\tau$ and $\ddot{x}^\mu \equiv d^2x^\mu/d\tau^2$). The value of $k = (E + 2K)/m_0c^2$ represents the total energy of the particle in its orbit. For a photon, under the same conditions, one gets:

$$\alpha \dot{t} = k, \tag{39}$$

$$\dot{r}^2 + \frac{h^2\alpha}{r^2} = c^2k^2 = c^2 + 2K, \tag{40}$$

$$r^2\dot{\phi} = -h, \tag{41}$$

where the derivatives are now expressed as a function of the affine parameter l. At smaller distances, the convergence of the *erfc* towards zero forces the system away from any singular divergence. Here is a short list of the main predictions resulting from this model [28]:

1. For particle radial trajectories, depending on the σ value, dr/dt will be smaller than Einstein's predictions and the coordinate time dt will be smaller than the proper time $d\tau$ when $r \to \infty$.
2. In equatorial orbits, contrary to Einstein's predictions, a free massive particle can maintain a circular orbit in that system, whatever its angular momentum. At a small scale, the effective potential V_{eff} does not fall down as Einstein predicted but keep on increasing like Newton's pattern. In other words, the present metric, as set out in Eq. (4), does not predict an unstable maximum or unstable inner circular orbit.
3. For photon radial trajectories, comparing with a Schwarzschild description, there is no discontinuity in the trajectory of outgoing or incoming photons since there are no coordinates or real singularities in such a system and the effect of the residual constant factor leads to predicting that the defined value of the speed of light is made up of two components (Eqs. 6, 12 and 13).
4. Concerning the photon's equatorial orbits, the main difference comes from the use of an *erfc* potential instead of the Newtonian limit, which eradicates the local maximum of the effective potential V_{eff} here again. As well, slight differences on the impact parameter are expected as compared to Einstein's predictions since the Newton potential is substituted by an *erfc* potential.

5. When the defined value of the speed of light c_d is used to mask the constant offset error of the *erfc* potential, the model reduces to an *erf* potential, a more familiar representation with one intrinsic and one coordinate singularities, but the absence of a full gravitational collapse makes the intrinsic singularity unreachable. Here is how it goes.

Gravitational collapse

A system described by the metric Eq. (4) will hardly experience unbounded gravitational collapse. Such a collapse is expected to happen, for example in white-dwarf stars, when the degenerated electron Fermi gas becomes relativistic. In this case, the gas cannot supply enough pressure to counterbalance gravitational forces. In other words, there is no stable equilibrium in the total energy, (no minimum as a function of the star radius r). Such a conclusion is not supported, however, if the full *erfc* potential is taken into account. In that case, for a star of mass M and of proper length σ, the extreme relativistic N electron gas will have a total energy of:

$$\frac{N^{4/3}(9\pi c^3\hbar^3/4)^{1/3}}{r}+\frac{\sqrt{\pi}GM^2}{\sigma\sqrt{2}}erfc\left(\frac{\sigma}{\sqrt{2}r}\right) \tag{42}$$

with a minimum at:

$$r_{\min}=\frac{\sigma}{\sqrt{2}}\left[\frac{-1}{\ln(\vartheta/GM^2)}\right]^{1/2} \tag{43}$$

where $\vartheta=N^{4/3}(9\pi c^3\hbar^3/4)^{1/3}$ if σ was constant throughout the process. According to the heuristics (10), this is certainly not the case and more complex stopping conditions are predicted. For example, combining (10) with (42), σ becomes proportional to r^4 and the derivative of (42) leads to a seventh order polynomial with multiple roots. In this case, the collapsing phenomenon would stop at the largest of these root $r_{\min\max}$. Depending on the masses involved, the escape velocity might however be greater than the speed of light, resulting in a black star phenomenon [29] which will create very large distortions in the surrounding space–time.

Moreover, for an observer working in c_d with the *erf* potential, the resulting intrinsic singularity at $r_{\text{int.sing}}=0$ will never be reached but the coordinate singularity will define an event horizon when $r_{\min\max}<r_{\text{coord.sing}}$.

To summarize, there are conditions for which a star with no gravitational collapse will have a horizon in a model based on an erf potential. Generally speaking, $r_{\min\max}$ decreases when M increases and $r_{\text{coord.sing}}$ increases when M increases, since erf decreases when $r_{\text{coord.sing}}$ increases and since erf decreases when M increases, so $r_{\text{coord.sing}}$ increases when M increases, which make the event horizon expectable in many conditions.

Discussion

Eqs. (1) and (2) predicts a convergence toward the Newtonian field at large distance but the potential is no longer defined up to a gauge transformation: for a given mass, it has a definite offset value which should be directly observable or at least manifest itself in some physical phenomena.

We have previously provided interesting effects of this hypothesis on various well-known phenomena [12]. It is at this observation level that the model has to be further tested, validated or rejected. For example, a detailed analysis of the *erfc* potential could be used:

1. To elucidate why the Sun's oblateness and quadrupole moments are smaller than the Newtonian predictions [30] since the sign of the third power term is opposite to the first power term in series expansion of the *erfc* potential while these two terms are of the same sign in the development of the Newtonian expression. The third term of the *erfc* series, as normalized in σ, is also smaller than its Newtonian analogue.
2. To develop new stellar interior models. The present diagonal metric, as set out in Eq. (4), is a solution to the field equations of a spherically symmetric massive system as seen from its interior. For an observer inside such a large system, the matter-energy extends from r equals zero to infinity.
3. To investigate particularly static high-density star models, massive objects with no intrinsic singularity at their centre, since the *erfc* potential stops any gravitational collapse, which in extreme cases might result in black stars, as superficially investigated in Section "Gravitational collapse".
4. To study anomalous phenomena reported in the Solar system [12], after expressing the actual symmetric metric in terms of a dynamic axisymmetric space–time geometry, [10] which will be the subject of a companion paper.

Conclusion

One key feature of the present model [31] is that it is based on the existence of an intrinsic star specific physical constant, the parameter σ^2. Incorporating the new *erfc* potential into a spherically symmetric metric, we have described various features of the resulting geometry and compared these to Einstein's classical predictions under similar conditions. In spite of its interesting and challenging viewpoints, the analogical and heuristic methodology previously used to justify the use of the erfc potential [31] remains an open problem and also raises many questions. Further mathematical developments will be necessary to completely formalize this theoretical model. So far, we have to proposed a paradigm [10] that would justify the emergence of such a potential but this approach is still weak and requires further developments, particularly if the model aims, in the long term, at bridging the gap between general relativity and quantum mechanics. This might require reconsidering the whole approach for example in the context of models that leads to non-singular black holes like 2D dilaton or other vacuum theories solvable both classically and quantum mechanically, as developed in [32,33], but this is beyond the scope of the present paper.

Finally one interesting remark regarding the present model is that it point out the potential impact of two historical decisions: fixing at zero the value of the gravitational potential at infinity and choosing the water as the reference mass to define the kilogram. Further investigations will be required to see in the resulting numerical predictions are just coincidental or lead to a more fundamental understanding of the observer's choices.

Acknowledgements

This work has been partly supported over the years by RGPIN discovery grants from NSERC Canada to Réjean Plamondon, as well as by the Department of Electrical Engineering, Polytechnique Montréal. The author thanks Claudéric Ouellet-Plamondon and André Laveau for their kind help with computer simulations and figure preparation.

References

[1] Barcelo C, Liberati S, Visser M. Analogue gravity. Living Rev Relativity 2011;14 (3).
[2] Faraoni V. Cosmology in scalar-tensor gravity (fundamental theories of physics). Dordrecht: Springer Sciences and Business Media; 2004.
[3] Sotiriou TP, Faraoni V. *f(R)* theories of gravity. Rev Mod Phys 2010;82:451.
[4] Capozziello S, De Laurentis M. Extended theories of gravity. Phys Rep 2011;509:167.

[5] Capoziello S, Faraoni V. Beyond Einstein gravity, a survey of gravitational theories for cosmology and astrophysics. Dorrdrecht: Springer; 2010.
[6] De Felice A, Tsujikawa S. Living Rev Relativity 2010;13:3. , https://doi.org/10.12942/lrr-2010-3.
[7] Clifton T, Ferreira PG, Padilla A, Skordis C. Modified gravity and cosmology. Phys Rep 2012;513:1–189.
[8] Franklin A, Fishbach E. The rise and fall of the fifth force: discovery, pursuit and justification in modern physics. 2nd ed. Springer; 2016.
[9] Capozziello S, De Laurentis M. Scholarpedia 2015;10(2):31422.
[10] Plamondon R, Ouellet Plamondon. Emergence of a quasi newtonian law of gravitation: a geometrical impact study. In: Rosquist K, Jantzen RT, Ruffini R, editors. Proc. of the thirteenth marcel Grossmann meeting on general relativity, on recent developments in theoretical and experimental general relativity, astrophysics, and relativistic field theories. Singapore: World Scientific; 2015.
[11] Hobson MP, Efstathiou G, Lasenby AN. General relativity an Introduction for physicists. Cambridge, U.K: Cambridge University Press; 2006.
[12] Plamondon R. Solar system anomalies: revisiting Hubble's law. Phys Essays 2017;30(4):403.
[13] Mohr PJ, Newell DB, Taylor BN. CODATA Recommended Values of the Fundamental Physical Constants: 2014, NIST Publication, September 26; 2016.
[14] "2016 Selected Astronomical Constants", The Astronomical Almanac Online, USNO–UKHO.
[15] Liu Y-C, Yang X-S, Zhu H-B, Zhou W-H, Wang Q-S, Zhao Z-Q, Jiang W-W, Wu C-Z. Testing non-Newtonian gravitation on a 320 m tower. Phys Lett A 1992;168:131–3.
[16] Romaides AJ, Sands RW, Eckhardt DH, Fischbach E, Talmadge CL, Kloor HT. Second tower experiment: further evidence for newtonian gravity. Phys Rev D 1994;50:3608–13.
[17] Yang S-Q, Zhan B-F, Wang Q-L, Shao C-G, Tu L-C, Tan W-T, et al. Test of the gravitational inverse square law at millimeter ranges. Phys Rev Lett 2012;108:081101.
[18] Will CM. The confrontation between general relativity and experiment. Living Rev Relativity 2014;17:4.
[19] Nobili AM, Will CM. The real value of Mercury's Perihelion advance. Nature 1986;320:39.
[20] Unzicker A. Why do we still believe in Newton's Law ? Facts, myths and methods in gravitational physics, arXiv:gr-qc/0702009v8; 2008.
[21] Villard R, Reiss A. Hubble Site, News Release Number STScI-2009-08; 2009.
[22] C Moskowitz, SPACE.com, http://www.space.com/17884-universe-expansion-speed-hubble-constant.html, (2012).
[23] Freedman WL, Madore BF, Scowcroft V, Burns C, Monson A, Persson SE, et al. Astrophys J 2012;758:24.
[24] Riess AG, Macri L, Casertano S, Lampeitl SH, Ferguson HC, Filipenko AV, et al. Astrophys J. 2011;730:119.
[25] Riess AG, Macri LM, Hoffmann SL, Scolnic D, Casertano S, Filippenko AV, et al. arXiv:1604.01424, (9 June 2016).
[26] Ricci G. Atti del Reale Istituto Veneto di Scienze. Lettere ed Arti 1904;53:1233.
[27] Kretschmann E. The principle determinability of the calculated framework of the arbitrary theory of relativity, part I. Ann Phys 1915;48: 907; part II. 1915;48.
[28] Plamondon R. Patterns in physics, toward a unifying theory, Montréal, Canada: Presses Internationales Polytechnique; 2012.
[29] Barcelo C, Liberati S, Sonego S, Visser M. Fate of gravitational collapse in semiclassical gravitation. Phys Rev D 2008;77(4):044032.
[30] Rozelot JP, Damiani C. History of solar oblateness measurements and interpretation. Eur Phys J H 2011;36:407–36.
[31] Plamondon R, O'Reilly C. Ouellet-plamondon, strokes against stroke—strokes for strides. Pattern Recogn 2014;44(3):929–44.
[32] Grumiller D, Kummer W, Vassilevich DV. Dilaton gravity in two dimensions. Phys Rept 2002;369:327–430.
[33] Kunstatter G, Maeda H, Taves T. New 2D Dilaton gravity for nonsingular black holes. Classical Quantum Gravity 2016;33(10).